

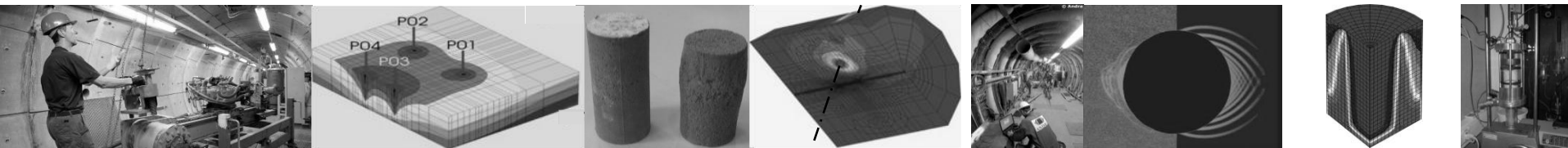
Transversal action “ Models “

Phase 3 : Underground structure modelling

B. Pardoen - F. Collin - S. Levasseur - R. Charlier

Université de Liège – ArGenCo

Andra - GL Geomechanics - September 2014



1. CONSTITUTIVE MODELS
2. MODELS FITTING
3. NUMERICAL MODELLING – TYPE 1
4. NUMERICAL MODELLING – FRACTURES MODELLING – TYPE 1 AND 2
5. CONCLUSIONS AND OUTLOOKS

1. **CONSTITUTIVE MODELS**
2. MODELS FITTING
3. NUMERICAL MODELLING – TYPE 1
4. NUMERICAL MODELLING – FRACTURES MODELLING – TYPE 1 AND 2
5. CONCLUSIONS AND OUTLOOKS

1. Constitutive models

1.1 Balance equations (LAGAMINE FE code) :

Momentum :

$$\text{div}(\sigma_{ij}) = 0$$

Bishop's effective stress :

$$\sigma_{ij} = \sigma'_{ij} - b_{ij} S_{r,w} p_w \delta_{ij}$$

Water mass :

$$\frac{\partial}{\partial t} (\rho_w \Phi S_{r,w}) + \text{div}(\rho_w \underline{q}_w) = 0$$

1.2 Flow model :

Advection of liquid phase (Darcy's flow) :

$$\underline{q}_w = - \frac{k_{ij} k_{r,w}(S_{r,w})}{\mu_w} \underline{\nabla} p_w$$

Water retention and permeability curves (Van Genuchten's model) :

$$S_{r,w} = S_{res} + (S_{max} - S_{res}) \left[1 + \left(\frac{p_c}{P_r} \right)^n \right]^{-m} \quad k_{r,w} = \sqrt{S_{r,w}} \left[1 - (1 - S_{r,w}^{1/m})^m \right]^2$$

Symbol	Name	Value	Unit
$k_{hor, //}$	Horizontal intrinsic water permeability	$4 \cdot 10^{-20}$	m^2
$k_{vert, \perp}$	Vertical intrinsic water permeability	$1.33 \cdot 10^{-20}$	m^2
Φ	Porosity	0.173	-
m	Van Genuchten coefficient	0.33	-
n	Van Genuchten coefficient	1.49	MPa
P_r	Van Genuchten parameter	15	MPa

1. Constitutive models

1.3 Mechanical model :

Elasto-viscoplasticity : $\epsilon_{ij} = \epsilon_{ij}^e + \epsilon_{ij}^p + \epsilon_{ij}^{vp}$

1.3.1 Linear elasticity theory :

Stress-strain relation, Hooke law : $d\epsilon_{ij}^e = D_{ijkl}^e d\sigma_{kl}'$, $d\sigma_{ij}' = C_{ijkl}^e d\epsilon_{kl}^e$, $C_{ijkl}^e = inv(D_{ijkl}^e)$

Orthotropic (9 param.) :

Cross-anisotropic (5 param.) :

Isotropic (2 param.) :

$E_1, E_2, E_3, \nu_{12}, \nu_{13}, \nu_{23}, G_{12}, G_{13}, G_{23}$

$E_{//}, E_{\perp}, \nu_{///}, \nu_{//\perp}, G_{//\perp}$

E, ν

$$D_{ijkl}^e = \begin{bmatrix} \frac{1}{E_1} & -\frac{\nu_{21}}{E_2} & -\frac{\nu_{31}}{E_3} & 0 & 0 & 0 \\ -\frac{\nu_{12}}{E_1} & \frac{1}{E_2} & -\frac{\nu_{32}}{E_3} & 0 & 0 & 0 \\ -\frac{\nu_{13}}{E_1} & -\frac{\nu_{23}}{E_2} & \frac{1}{E_3} & 0 & 0 & 0 \\ 0 & 0 & 0 & \frac{1}{2G_{12}} & 0 & 0 \\ 0 & 0 & 0 & 0 & \frac{1}{2G_{13}} & 0 \\ 0 & 0 & 0 & 0 & 0 & \frac{1}{2G_{23}} \end{bmatrix}$$

$$D_{ijkl}^e = \begin{bmatrix} \frac{1}{E_{//}} & -\frac{\nu_{///}}{E_{//}} & -\frac{\nu_{\perp//}}{E_{\perp}} & 0 & 0 & 0 \\ -\frac{\nu_{///}}{E_{//}} & \frac{1}{E_{//}} & -\frac{\nu_{\perp//}}{E_{\perp}} & 0 & 0 & 0 \\ -\frac{\nu_{//\perp}}{E_{//}} & -\frac{\nu_{//\perp}}{E_{//}} & \frac{1}{E_{\perp}} & 0 & 0 & 0 \\ 0 & 0 & 0 & \frac{1+\nu_{///}}{E_{//}} & 0 & 0 \\ 0 & 0 & 0 & 0 & \frac{1}{2G_{//\perp}} & 0 \\ 0 & 0 & 0 & 0 & 0 & \frac{1}{2G_{//\perp}} \end{bmatrix}$$

$$D_{ijkl}^e = \frac{1}{E} \begin{bmatrix} 1 & -\nu & -\nu & 0 & 0 & 0 \\ -\nu & 1 & -\nu & 0 & 0 & 0 \\ -\nu & -\nu & 1 & 0 & 0 & 0 \\ 0 & 0 & 0 & 1+\nu & 0 & 0 \\ 0 & 0 & 0 & 0 & 1+\nu & 0 \\ 0 & 0 & 0 & 0 & 0 & 1+\nu \end{bmatrix}$$

$\frac{\nu_{21}}{E_2} = \frac{\nu_{12}}{E_1}$, $\frac{\nu_{31}}{E_3} = \frac{\nu_{13}}{E_1}$, $\frac{\nu_{23}}{E_2} = \frac{\nu_{32}}{E_3}$

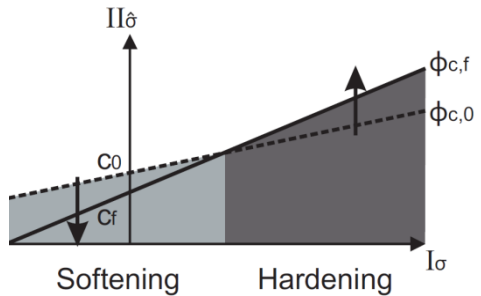
$\frac{\nu_{\perp//}}{E_{\perp}} = \frac{\nu_{//\perp}}{E_{//}}$

1. Constitutive models

1.3.2 Plasticity theory :

- Non-associated, elasto-viscoplastic, internal friction model.

Van Eeckelen yield surface :
$$F \equiv II_{\hat{\sigma}} - m \left(I_{\sigma} + \frac{3c}{\tan \phi_C} \right) = 0$$



- Hardening/softening of ϕ/c as a function of the Von Mises equivalent plastic strain :

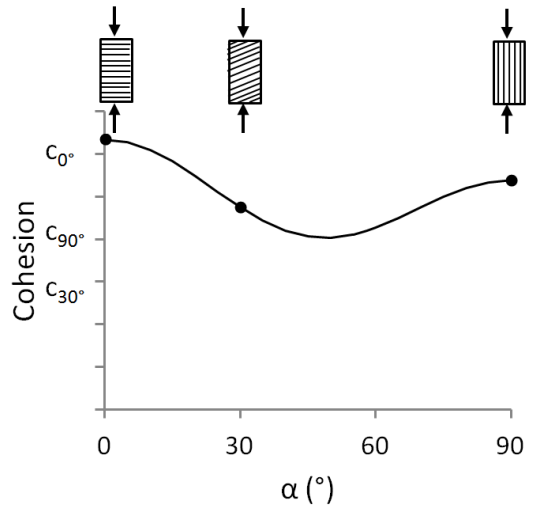
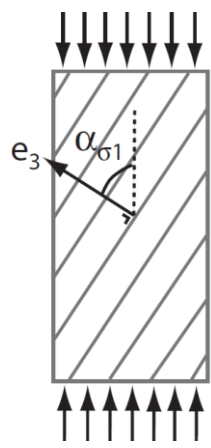
$$\varepsilon_{eq}^p = \sqrt{\frac{2}{3} \hat{\varepsilon}_{ij}^p \hat{\varepsilon}_{ij}^p} \quad \text{if } \varepsilon_{eq}^p > dec_{\phi} : \phi_C = \phi_{C0} + \frac{(\phi_{Cf} - \phi_{C0}) \cdot (\varepsilon_{eq}^p - dec_{\phi})}{B_{\phi} + (\varepsilon_{eq}^p - dec_{\phi})}$$

- Cohesion anisotropy by microstructure fabric tensor :

$$c = a_{ij} l_i l_j \quad , \quad l_i = \sqrt{\frac{\sigma_{i1}^2 + \sigma_{i2}^2 + \sigma_{i3}^2}{\sigma_{ij} \sigma_{ij}}}$$

For cross-anisotropy :

$$c = c_0 \left(1 + A_{11} (1 - 3l_2^2) + B_{11} A_{11}^2 (1 - 3l_2^2)^2 + \dots \right)$$



1. Constitutive models

1.3.3 Viscoplasticity theory :

- Loading surface of the viscoplastic flow : $f_{vp} = \sqrt{3}II_{\dot{\epsilon}} - \alpha_{vp} R_c \sqrt{A \left(C_s + \frac{I_{\sigma}}{3R_c} \right)} \geq 0$
- Viscoplastic hardening function : $\alpha_{vp} = \alpha_{vp,0} + (1 - \alpha_{vp,0}) \frac{\gamma_{vp}}{B_{vp} + \gamma_{vp}}$
- Equivalent viscoplastic shear strain : $\dot{\gamma}_{vp} = \sqrt{\frac{2}{3} \dot{\epsilon}_{ij}^{vp} \dot{\epsilon}_{ij}^{vp}}$

from Zhou et al. (2008), Jia et al. (2008)

1.3.4 Biot's coefficient anisotropy :

Biot's symmetric tensor : $b_{ij} = \delta_{ij} - \frac{C_{ijkk}^e}{3K_s}$

Orthotropic (3 param.) :

$$b_{ij} = \begin{bmatrix} b_{11} & & \\ & b_{22} & \\ & & b_{33} \end{bmatrix}$$

Cross-anisotropic (2 param.) :

$$b_{ij} = \begin{bmatrix} b_{//} & & \\ & b_{\perp} & \\ & & b_{//} \end{bmatrix}$$

Isotropic (1 param.) :

$$b_{ij} = \begin{bmatrix} b & & \\ & b & \\ & & b \end{bmatrix} = b \delta_{ij}$$
$$b = 1 - \frac{K_0}{K_s}$$

1. CONSTITUTIVE MODELS
- 2. MODELS FITTING**
3. NUMERICAL MODELLING – TYPE 1
4. NUMERICAL MODELLING – FRACTURES MODELLING – TYPE 1 AND 2
5. CONCLUSIONS AND OUTLOOKS

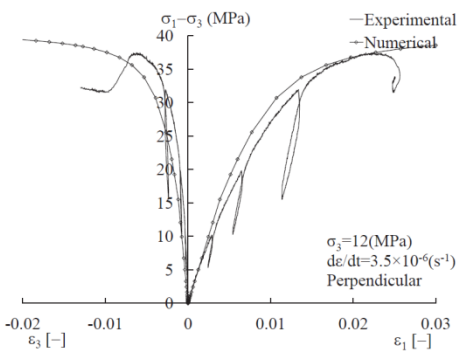
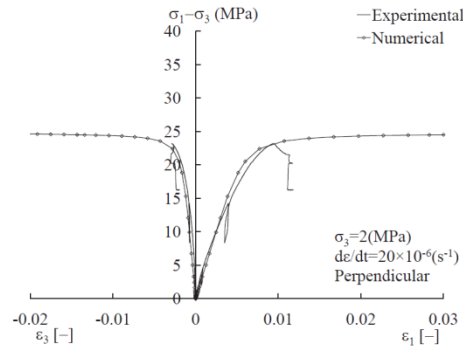
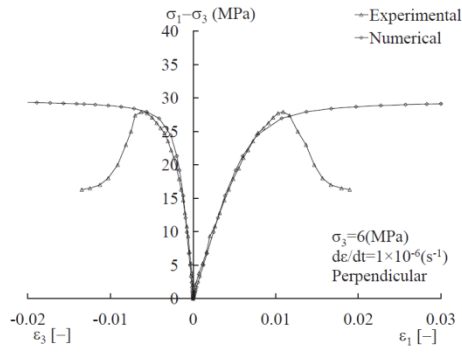
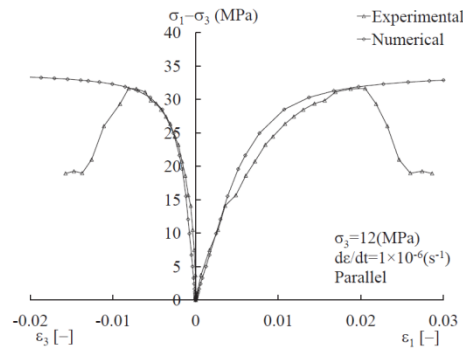
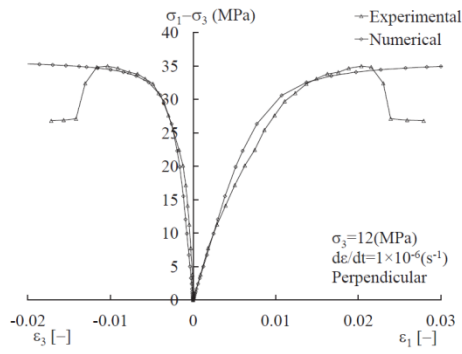
2. Models fitting

2.1 Triaxial compression tests :

Isotropic model

Elastoplastic, undrained condition

Symbol	Name	Value	Unit
E	Young's modulus	4000	MPa
v	Poisson's ratio	0.3	-
b	Biot's coefficient	0.6	-
ρ_s	Specific mass	2750	kg/m ³
ψ	Dilatancy angle	0.5	°
φ_{c0}	Initial compression friction angle	10	°
φ_{cf}	Final compression friction angle	23	°
B_φ	Friction angle hardening coefficient	0.001	-
dec_φ	Friction angle hardening shifting	0	-
c	Cohesion	4.2	MPa



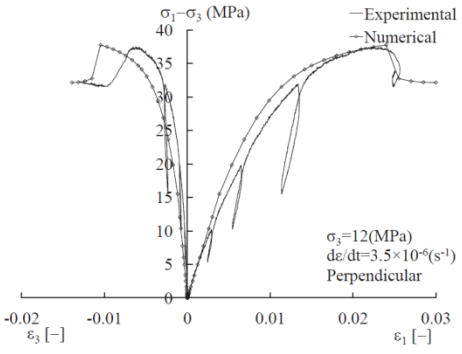
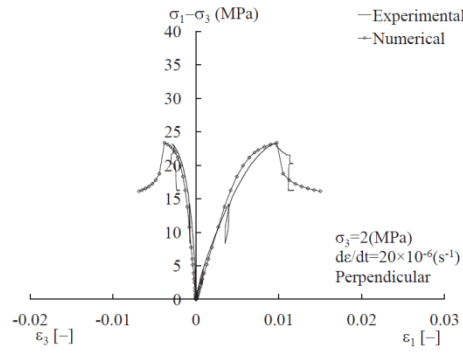
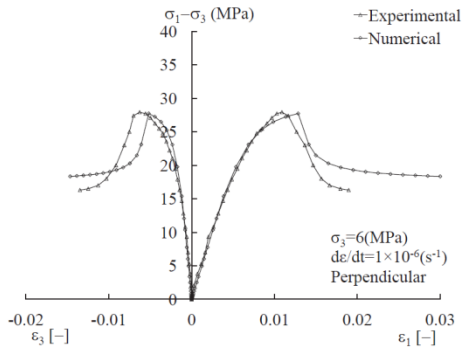
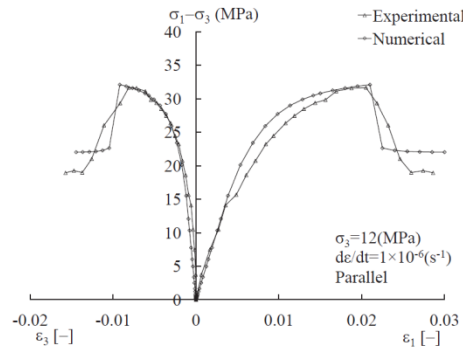
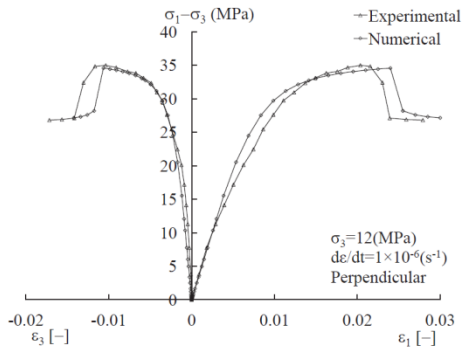
2. Models fitting

2.1 Triaxial compression tests :

Isotropic model

Elastoplastic, undrained condition

Symbol	Name	Value	Unit
E	Young's modulus	4000	MPa
ν	Poisson's ratio	0.3	-
b	Biot's coefficient	0.6	-
ρ_s	Specific mass	2750	kg/m ³
ψ	Dilatancy angle	0.5	°
ϕ_{c0}	Initial compression friction angle	10	°
ϕ_{cf}	Final compression friction angle	23	°
B_ϕ	Friction angle hardening coefficient	0.001	-
dec_ϕ	Friction angle hardening shifting	0	-
c_0	Initial cohesion	4.2	MPa
c_f	Final cohesion	0.04-2	MPa
B_c	Cohesion softening coefficient	0.001	-
dec_c	Cohesion softening shifting	0.011	-



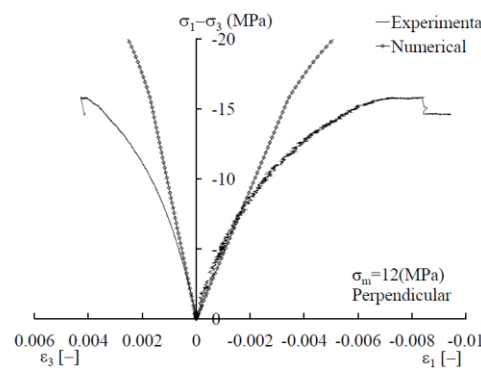
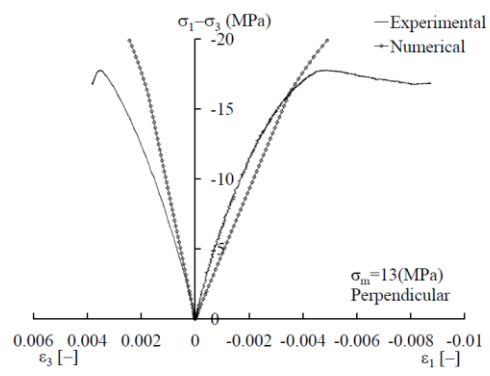
2. Models fitting

2.2 Triaxial extension tests :

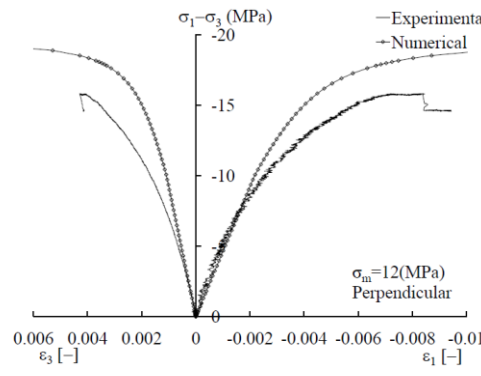
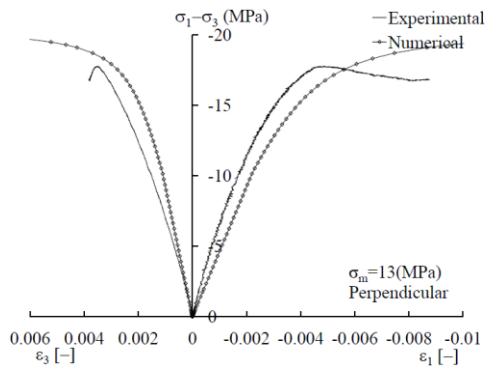
Isotropic model

Elastoplastic, undrained condition,
 $\rho = \text{cst}$, extension axiale

Symbol	Name	Value	Unit
E	Young's modulus	4000	MPa
ν	Poisson's ratio	0.3	-
b	Biot's coefficient	0.6	-
ρ_s	Specific mass	2750	kg/m ³
ψ	Dilatancy angle	0.5	°
φ_{c0}	Initial compression friction angle	10	°
φ_{cf}	Final compression friction angle	23	°
φ_{e0}	Initial extension friction angle	7	°
φ_{ef}	Final extension friction angle	23	°
B_φ	Friction angle hardening coefficient	0.001	-
dec_φ	Friction angle hardening shifting	0	-
c_0	Initial cohesion	4.2	MPa



Drucker-Prager



Van Eeckelen

Lower resistance in extension

2. Models fitting

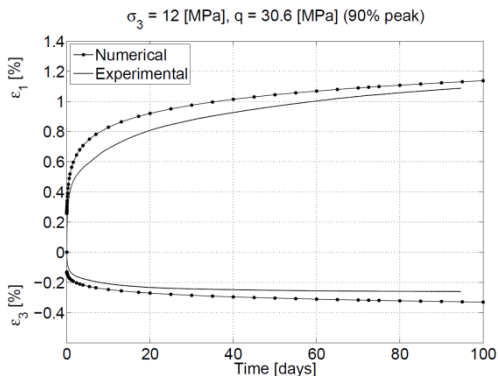
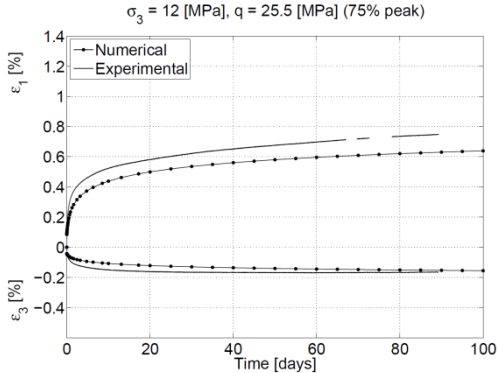
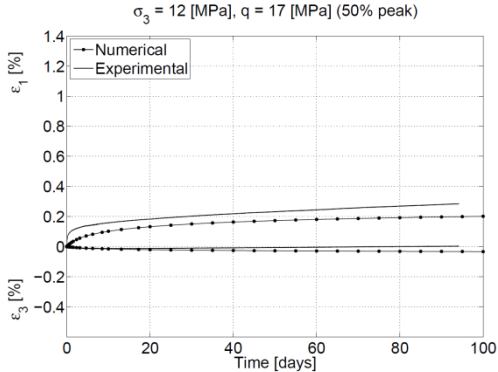
2.3 Creep tests :

Isotropic model

Elasto-viscoplastic, drained condition

$$f_{vp,0}=0$$

	Symbol	Name	Global fitting	Unit
Test description	RH	Laboratory Relative humidity	LAEGO 90	%
	σ_3	Confining pressure	12	MPa
	$\sigma_1 - \sigma_3$	Stress deviator	17, 25.5, 30.6	MPa
Plastic model	R_c	Uniaxial compression strength	21	MPa
	A	Internal friction coefficient	2.62	—
	C_s	Cohesion coefficient	0.03	—
	B_p	Plastic hardening function parameter	3.0×10^{-5}	—
	β_p	Compressibility/dilatancy parameter	1.1	—
Viscoplastic model for $f_{vp,0} = 0$	$\alpha_{vp,0}$	Initial threshold for the viscoplastic flow	0.142	—
	A_0	Reference fluidity	700	s^{-1}
	ζ	Temperature parameter	57×10^3	J/mol
	n	Creep curve shape parameter	5.0	—
	B_{vp}	Viscoplastic hardening function parameter	7.5×10^{-3}	—



2. Models fitting

2.4 Anisotropic parameters :

- Cross-anisotropic elasticity : $E_{//} = 5$ [GPa] , $E_{\perp} = 4$ [GPa] , $\nu_{///} = \nu_{//\perp} = 0.3$, $G_{//\perp} = 1.92$ [GPa]

- Biot : $b_{//} = 0.60$, $b_{\perp} = 0.66$

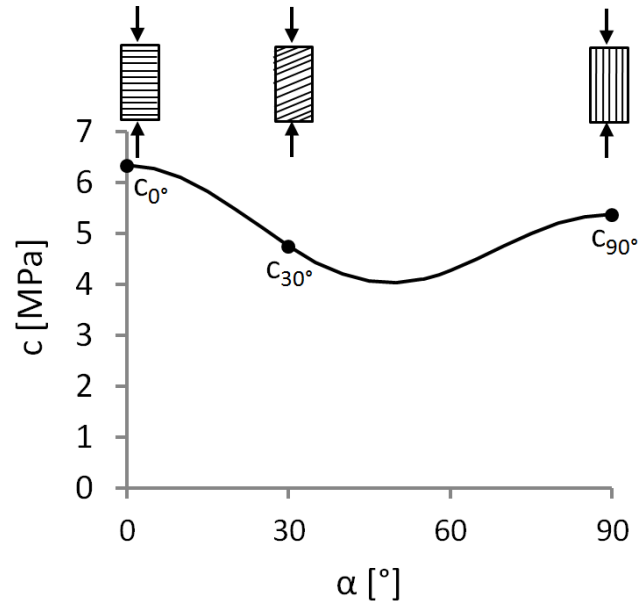
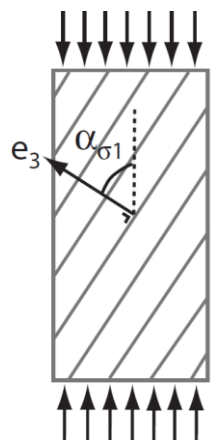
- Cohesion : $c_0 = 4.1$ [MPa] , $A_{11} = 0.117$, $B_1 = 14.24$

Cross-anisotropy $c = c_0 (1 + A_{11}(1 - 3l_2^2) + B_1 A_{11}^2 (1 - 3l_2^2)^2 + \dots)$

Uniaxial compression $l_2 = \cos(\alpha)$

Orientation [°]	0° (⊥)	30°	90° (//)
$R_{c,mean}$ [MPa] ¹	23.5	18.7	20.6
c' [MPa]	6.3	4.8	5.4

$$c' = \left(\frac{1 - \sin \varphi'}{2 \sin \varphi'} R_c + b S_{rv} p_w \right) \tan \varphi'$$



¹ Projet HAVL – Argile « Expertise sur les mesures sur échantillons d'argilite du module de déformation et de la résistance à la compression simple », Ref.: C.RP.0ULg.08.001, 2008

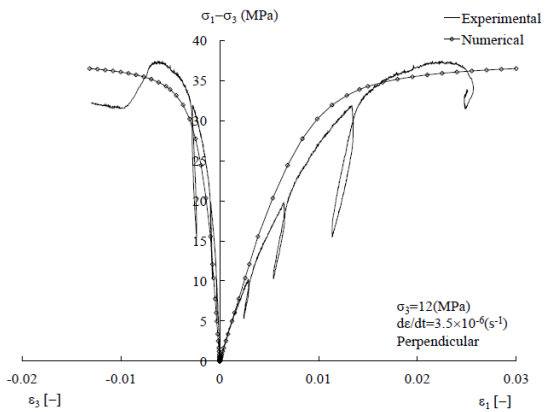
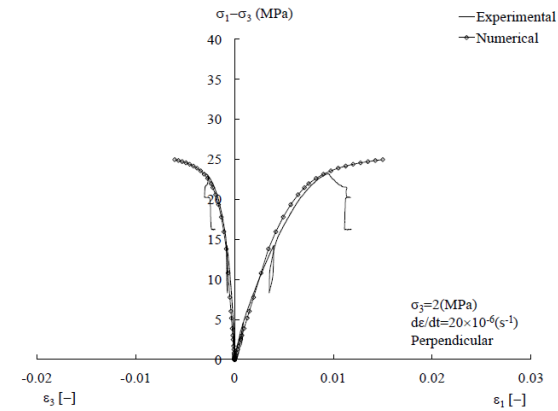
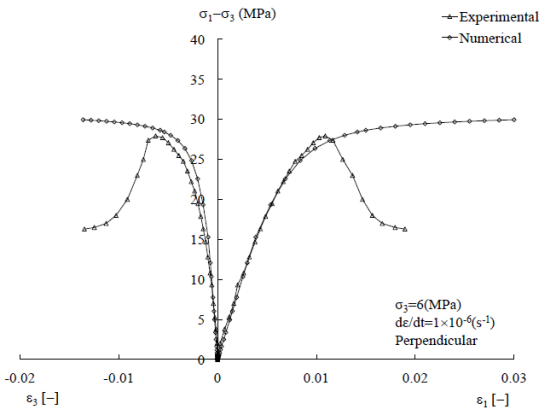
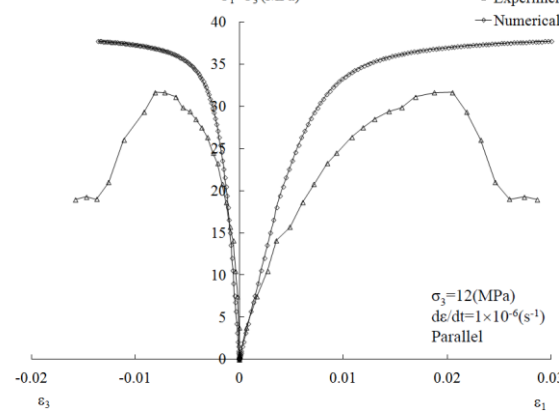
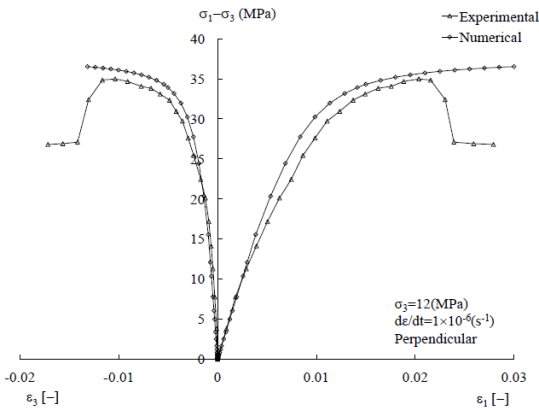
2. Models fitting

2.4 Anisotropic parameters :

Anisotropic model

Triaxial compression tests

Average values



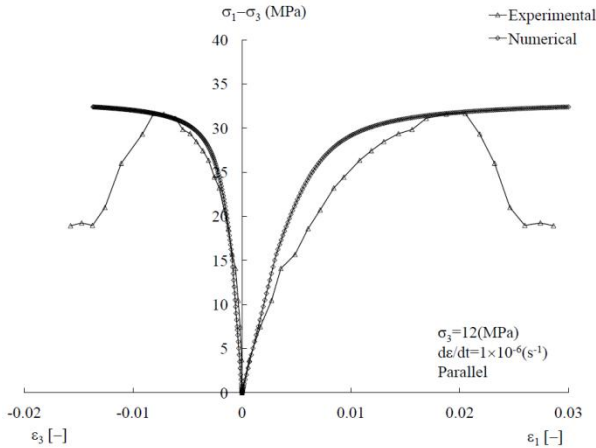
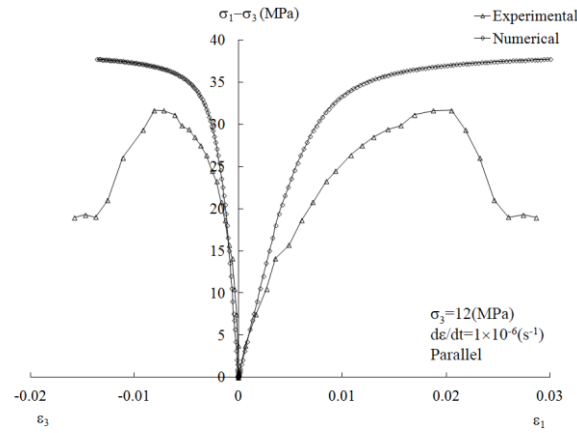
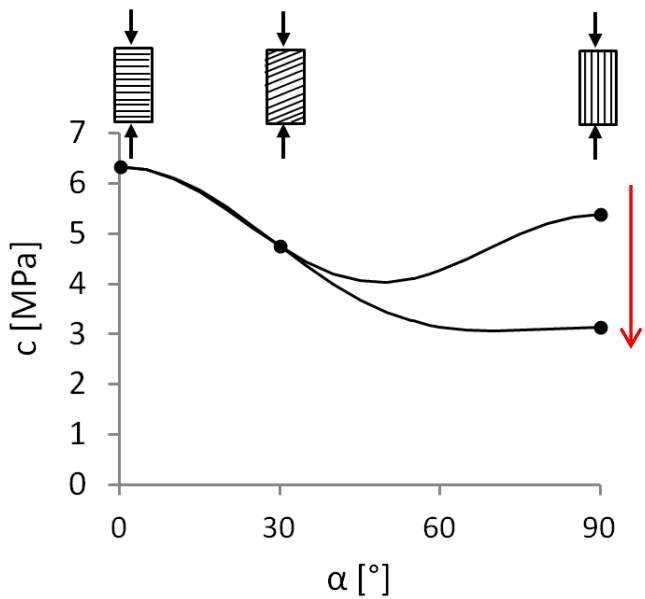
2. Models fitting

2.4 Anisotropic parameters :

Anisotropic model

Triaxial compression test

Average values



1. CONSTITUTIVE MODELS
2. MODELS FITTING
- 3. NUMERICAL MODELLING – TYPE 1**
4. NUMERICAL MODELLING – FRACTURES MODELLING – TYPE 1 AND 2
5. CONCLUSIONS AND OUTLOOKS

3. Numerical modelling – Galery type 1

3.1. Mesh / Boundary conditions / Initial conditions :

- Mesh :

By symmetry: quarter of the gallery.
 Modelling in 2D plane strain state.
 Gallery radius = 2.6 m.

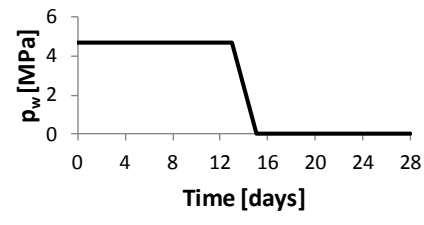
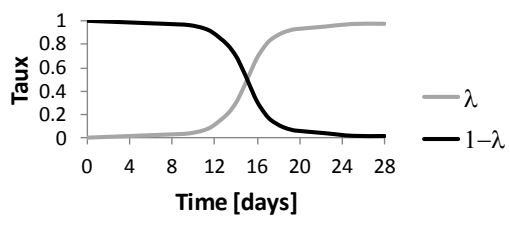
- Initial anisotropic stress state :

$$\begin{aligned}
 p_{w,0} &= 4.7 \text{ [Mpa]} \\
 \sigma_h = \sigma_z &= 12.40 \text{ [MPa]} \\
 \sigma_v = \sigma_y &= 12.70 \text{ [MPa]} \\
 \sigma_H = \sigma_x &= 1.3 \sigma_h = 16.12 \text{ [MPa]}
 \end{aligned}$$

- Hydraulic permeability anisotropy

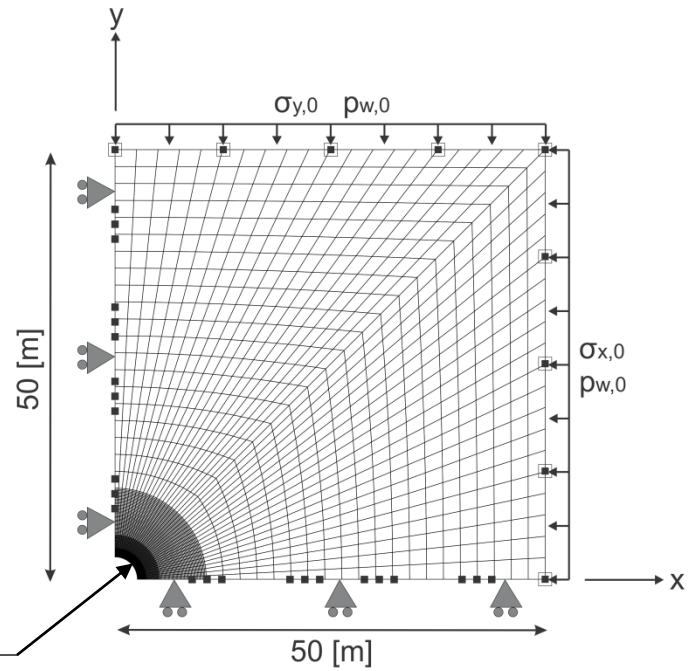
$$k_{\text{hor/vert}} = 4 \cdot 10^{-20} / 1.33 \cdot 10^{-20} \text{ [m}^2\text{]}$$

- Excavation :



- ▣ Constant pore water pressure ($p_{w,0}$)
- ← Constant total stress ($\sigma_{y,0} / \sigma_{x,0}$)
- ▶ Constrained displacement perpendicular to the boundary
- Impervious boundary

Nodal Points : 12281
 Elements : 4080



3. Numerical modelling – Galery type 1

3.2. Isotropic model :

3.2.1 Hydromechanical modelling, case 1.3 :

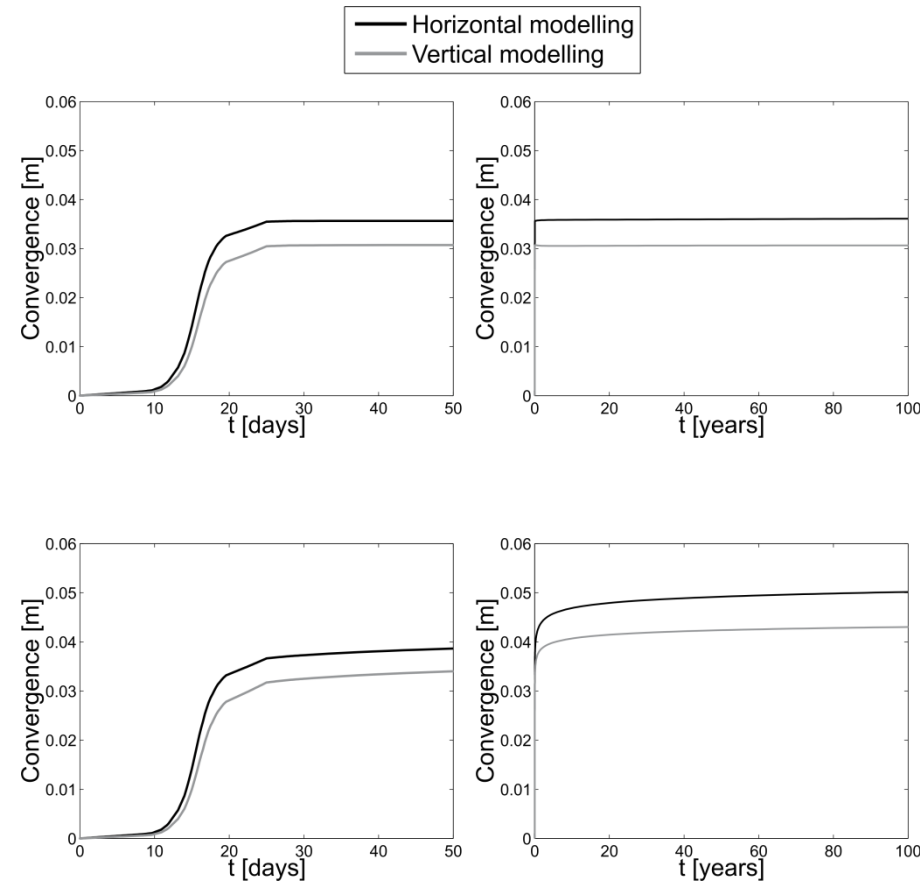
- Convergence + influence of viscosity :

(a) no viscosity

No evolution of deformation in the long term.

$$\sigma_H > \sigma_V, \epsilon_H > \epsilon_V$$

(b) viscosity



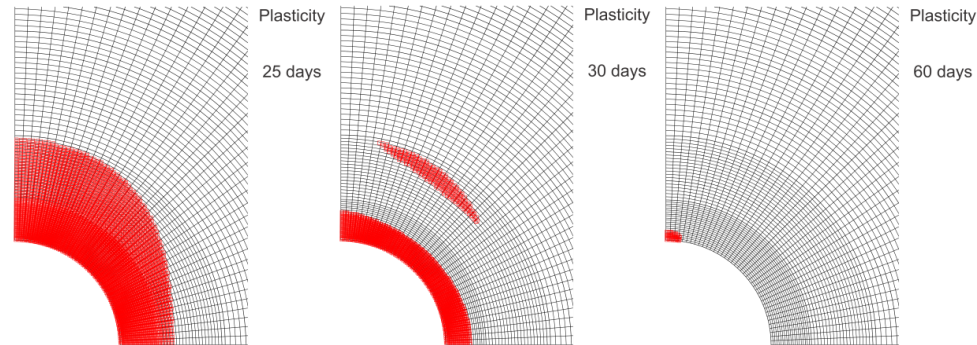
3. Numerical modelling – Galery type 1

3.2. Isotropic model :

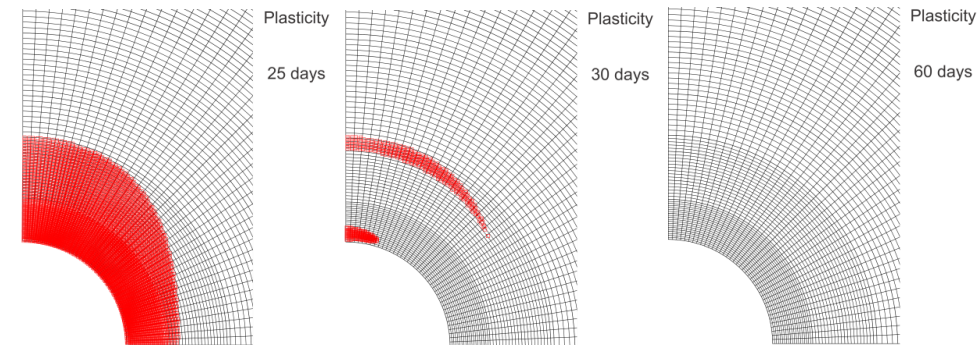
3.2.1 Hydromechanical modelling, case 1.3 :

- Plastic zone + influence of viscosity :

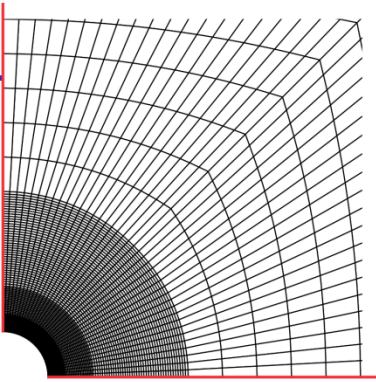
(a) no viscosity
HM coupling effect



(b) viscosity
HM coupling + viscosity effects



3. Numerical modelling – Galery type 1

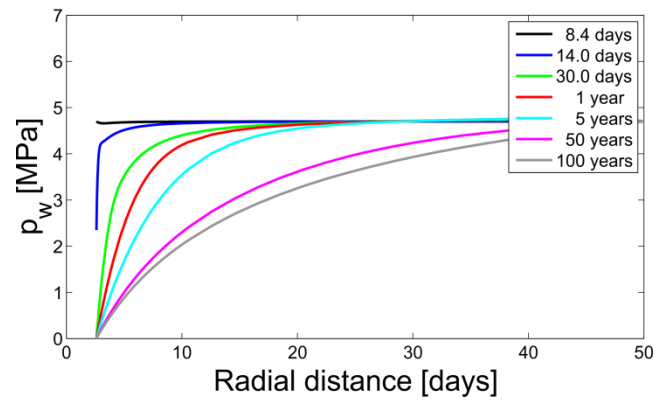


3.2. Isotropic model :

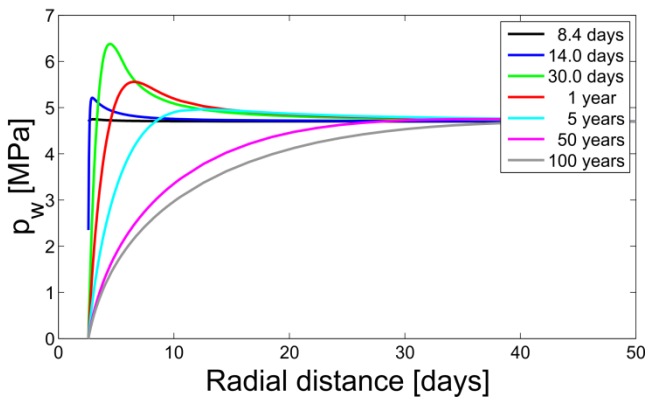
3.2.1 Hydromechanical modelling, case 1.3 :

- Pore water pressure :

Horizontal cross-section



Vertical cross-section



3. Numerical modelling – Galery type 1

3.2. Isotropic model :

3.2.2 Mechanical modelling, case 1.1 and 1.2 :

- Convergence + influence of the support :

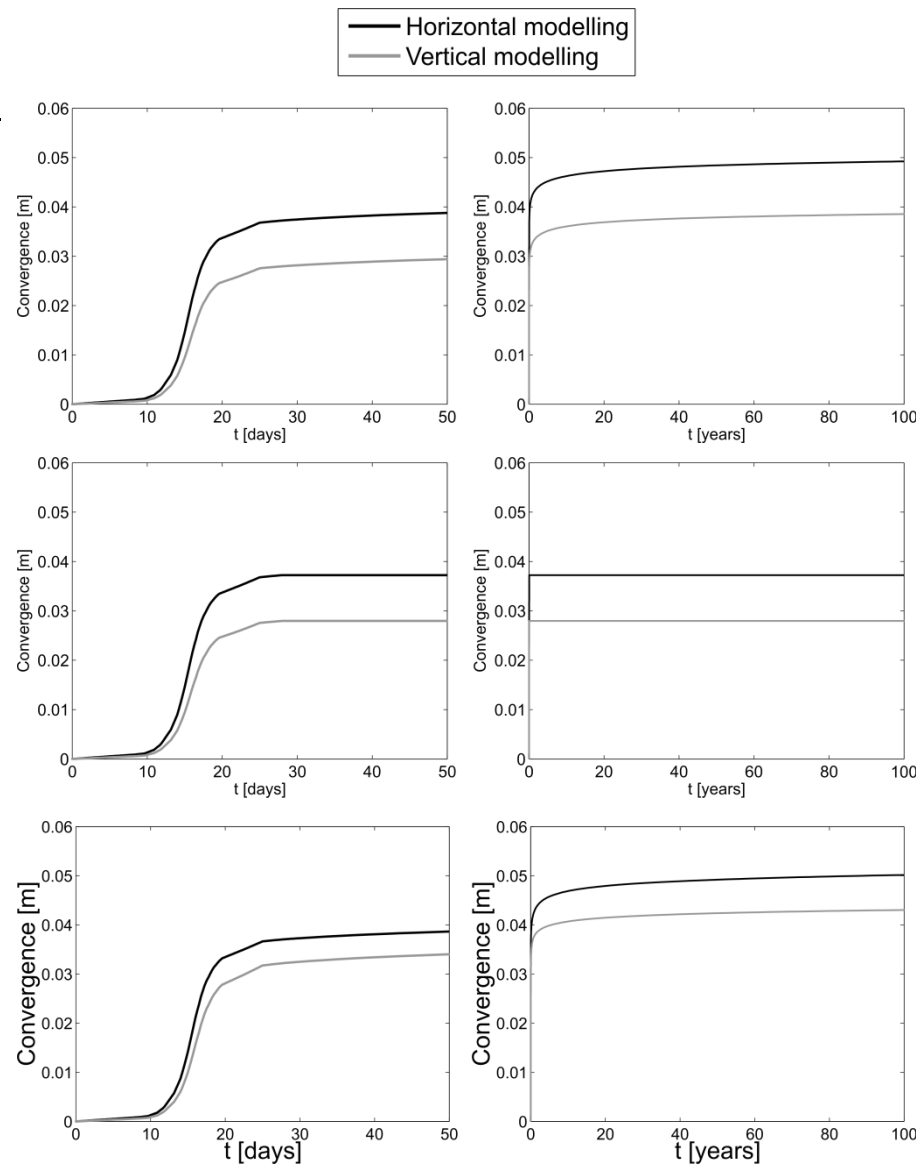
(a) Case 1.1, flexible liner

(b) Case 1.2, rigid liner

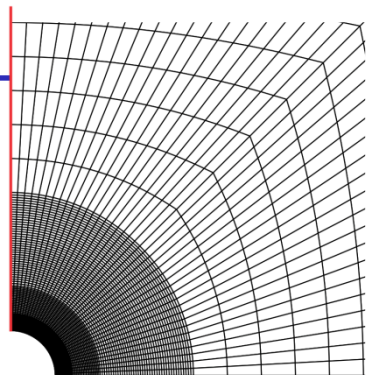
Stops the convergence after the excavation.

(c) Case 1.3, flexible liner, HM modelling

Similar to mechanical modelling in the long term.
Vertical convergence slightly greater.



3. Numerical modelling – Galery type 1



3.2. Isotropic model :

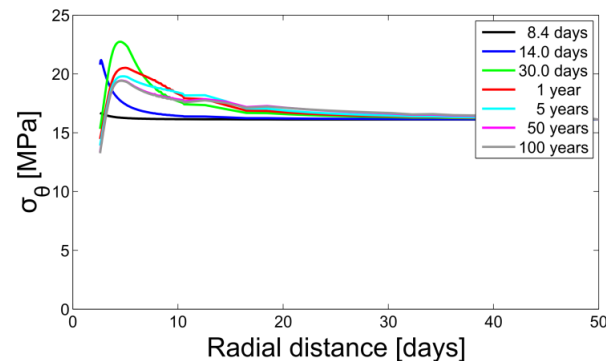
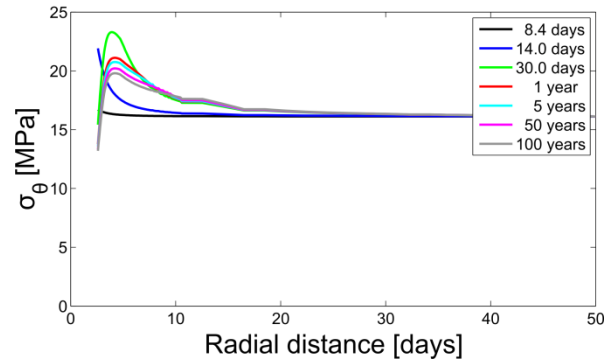
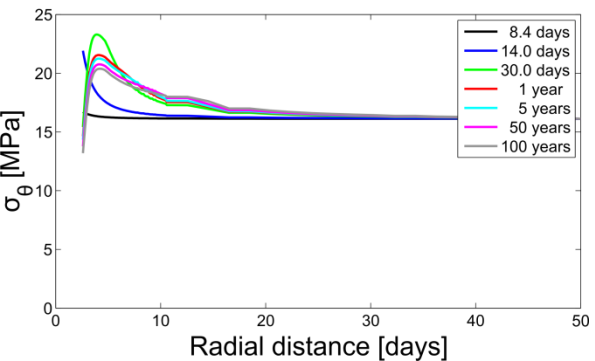
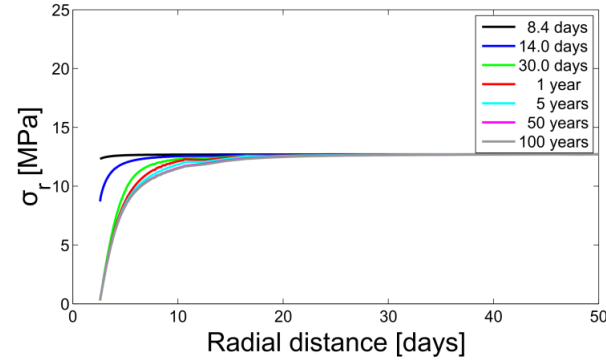
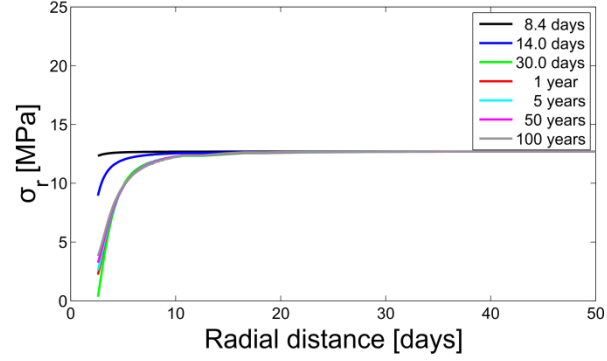
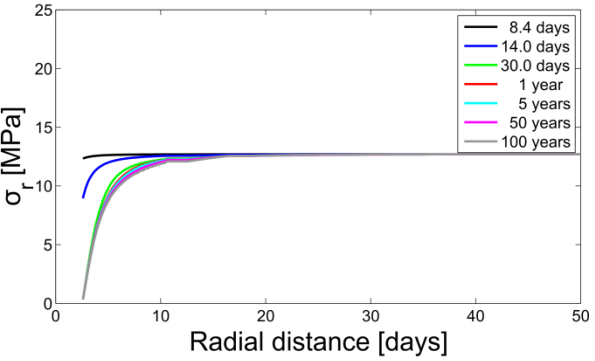
3.2.2 Mechanical modelling, case 1.1 and 1.2 :

- Radial and orthoradial total stress :
Vertical cross-section

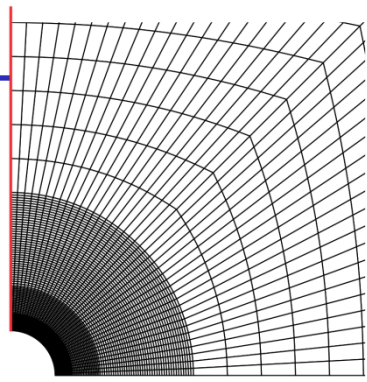
(a) Case 1.1, flexible liner
M modelling

(b) Case 1.2, rigid liner
M modelling

(c) Case 1.3, flexible liner
HM modelling



3. Numerical modelling – Galery type 1

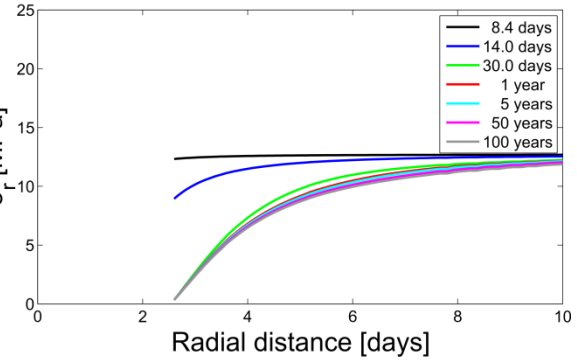


3.2. Isotropic model :

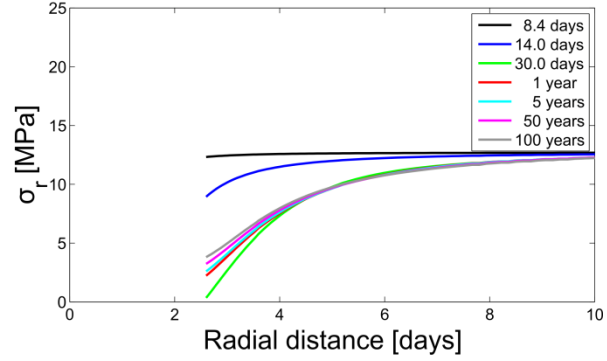
3.2.2 Mechanical modelling, case 1.1 and 1.2 :

- Radial and orthoradial total stress :
Vertical cross-section

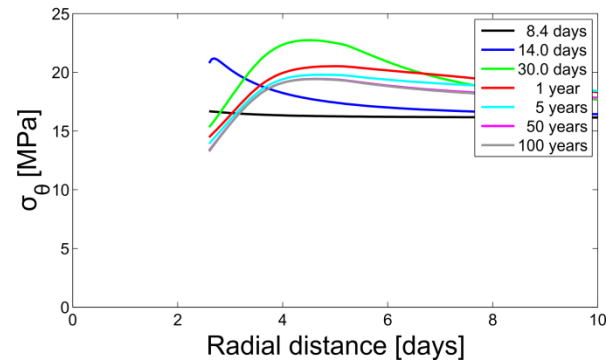
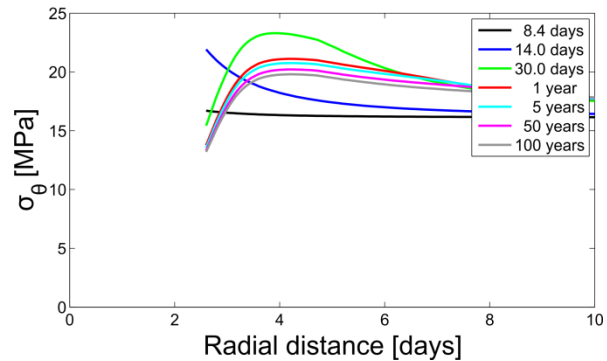
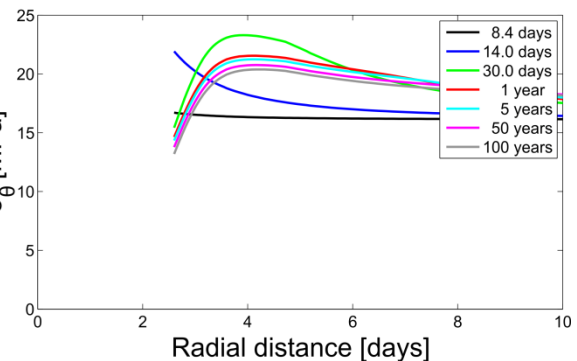
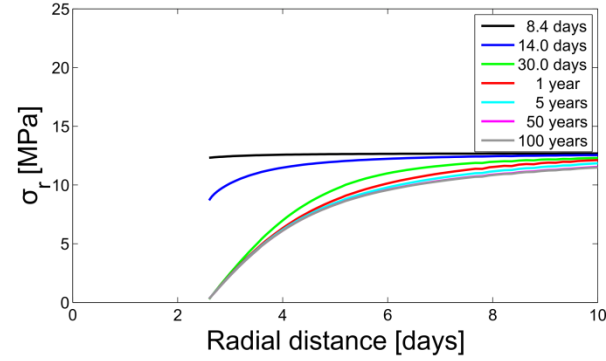
(a) Case 1.1, flexible liner
M modelling



(b) Case 1.2, rigid liner
M modelling



(c) Case 1.3, flexible liner
HM modelling



3. Numerical modelling – Galery type 1

3.3. Anisotropic model :

- Convergence + influence of the support :

(a) Case 1.1, flexible liner, M modelling

$$\sigma_H > \sigma_V, \epsilon_H > \epsilon_V$$

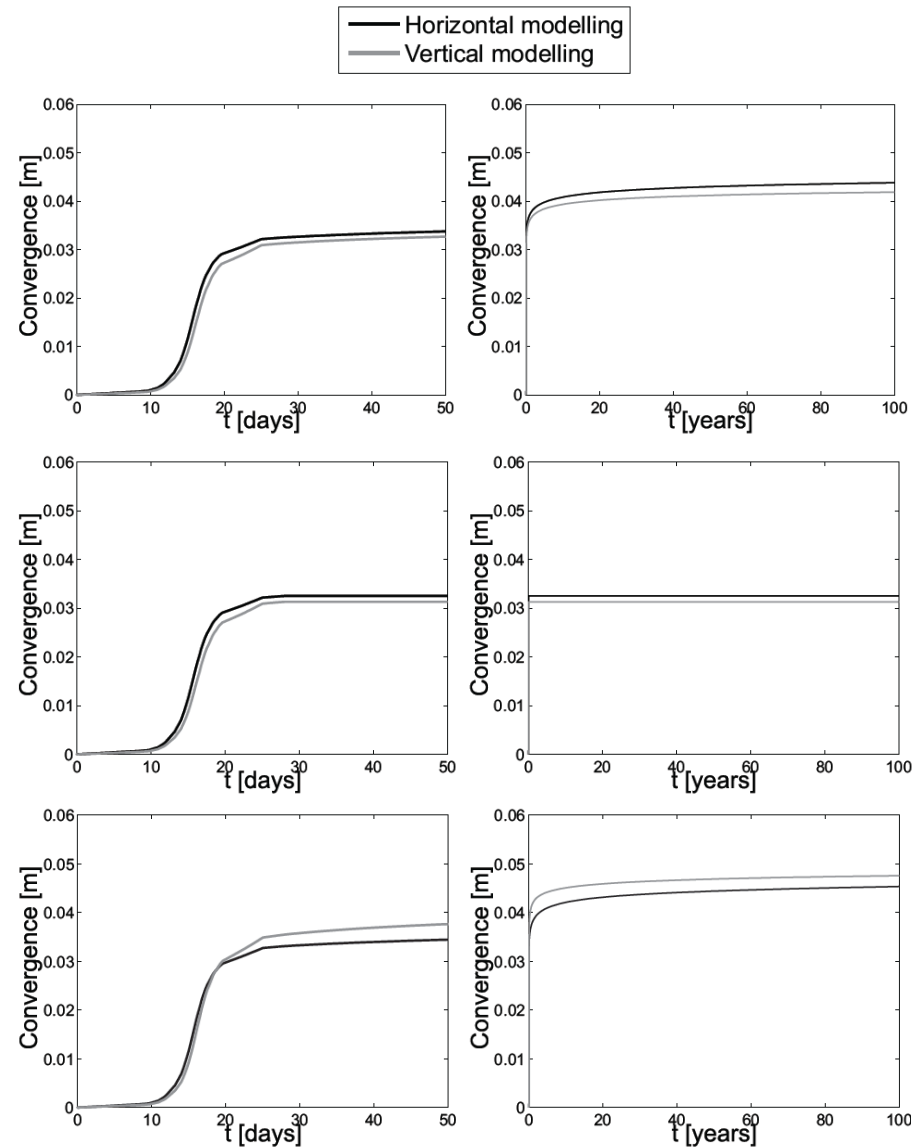
$$E_{//,hor} > E_{\perp,vert}, \epsilon_H < \epsilon_V$$

(b) Case 1.2, rigid liner, M modelling

Stops the convergence after the excavation.

(c) Case 1.3, flexible liner, HM modelling

Vertical convergence is greater than horizontal one.
This is due to the coupling !



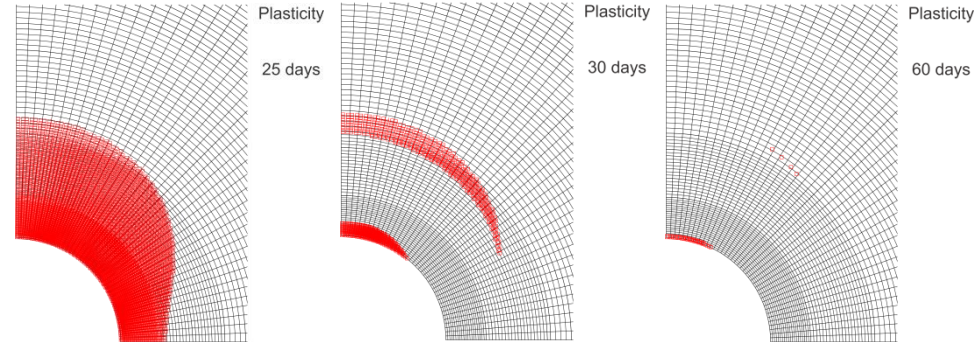
3. Numerical modelling – Gallery type 1

3.3. Anisotropic model :

- Plastic zone + influence of the support :

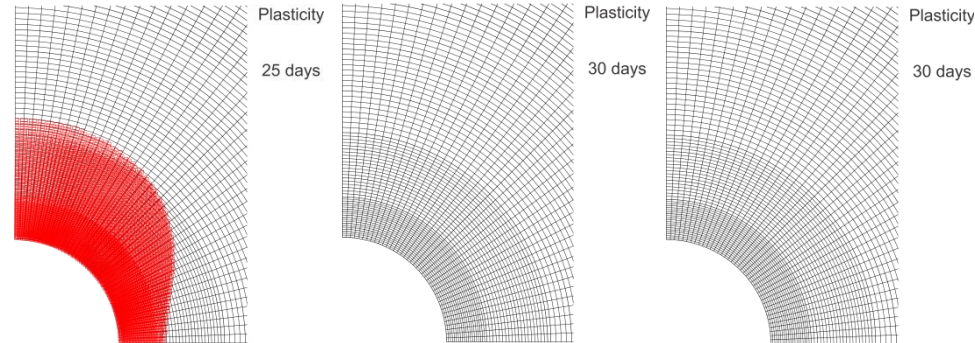
(a) Case 1.1, flexible liner, M modelling

Viscosity effects



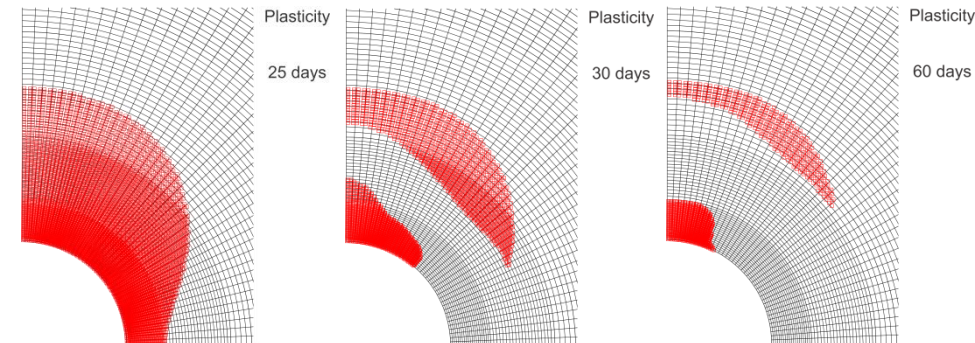
(b) Case 1.2, rigid liner, M modelling

Viscosity effects



(c) Case 1.3, flexible liner, HM modelling

HM coupling + viscosity effects



1. CONSTITUTIVE MODELS
2. MODELS FITTING
3. NUMERICAL MODELLING – TYPE 1
4. **NUMERICAL MODELLING – FRACTURES MODELLING – TYPE 1 AND 2**
5. CONCLUSIONS AND OUTLOOKS

4. Numerical modelling – Fractures modelling

4.1 Fracture modelling – strain localisation – coupled 2^d gradient model : (Chambon *et al.*, 1998 and 2001)

The continuum is enriched with microstructure effects. The kinematics include the classical one (macro) and the microkinematics (Toupin 1962, Mindlin 1964, Germain 1973).

Biphasic porous media : solid + fluid (Collin *et al.*, 2006)

$$\text{Balance equations : } \int_{\Omega} \left(\sigma_{ij} \frac{\partial u_i^*}{\partial x_j} + \underline{\Sigma_{ijk} \frac{\partial^2 u_i^*}{\partial x_j \partial x_k}} \right) d\Omega = \int_{\Omega} G_i u_i^* d\Omega + \int_{\Gamma_{\sigma}} \left(\bar{t}_i u_i^* + \underline{\bar{T}_i D u_i^*} \right) d\Gamma$$
$$\int_{\Omega} \left(\frac{\partial M}{\partial t} p_w^* - m_i \frac{\partial p_w^*}{\partial x_i} \right) d\Omega = \int_{\Omega} Q p_w^* d\Omega + \int_{\Gamma_q} \bar{q} p_w^* d\Gamma$$

Σ_{ijk} is the double stress, which needs an additional constitutive law = linear elastic law (Mindlin, 1964) function of the (micro) second gradient of displacement field :

$$\tilde{\Sigma}_{ijk} \left(\underline{D, \frac{\partial^2 u_i}{\partial x_j \partial x_k}} \right)$$

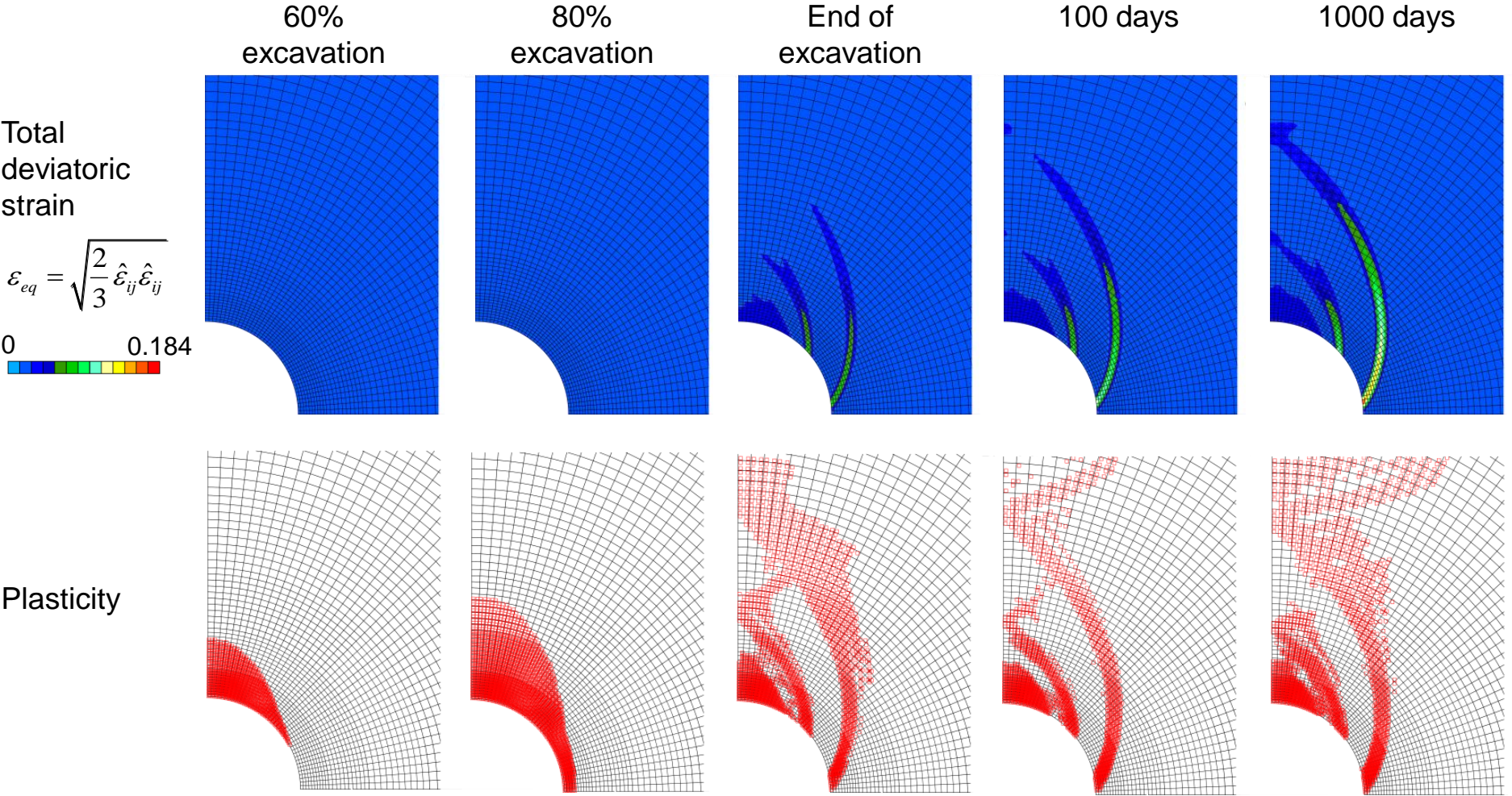
It depends only on one elastic parameter D . The internal length scale is related to this parameter.

(Chambon *et al.*, 1998, Kotronis *et al.*, 2007)

4. Numerical modelling – Fractures modelling

4.2 Galery type 1 - Hydromechanical modelling :

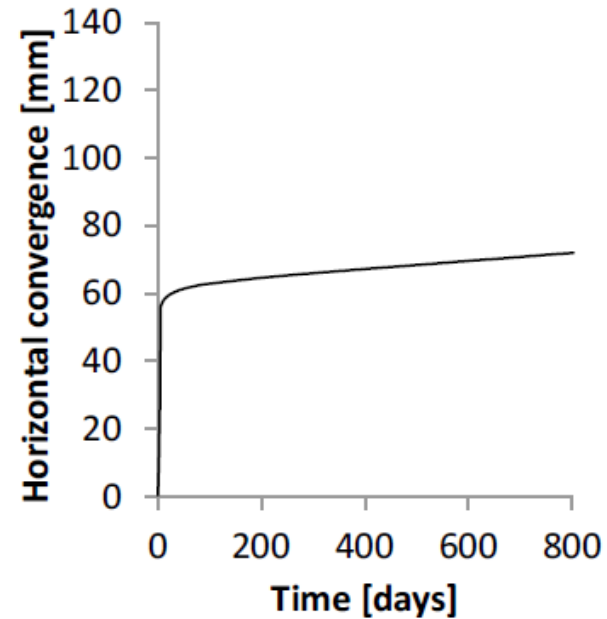
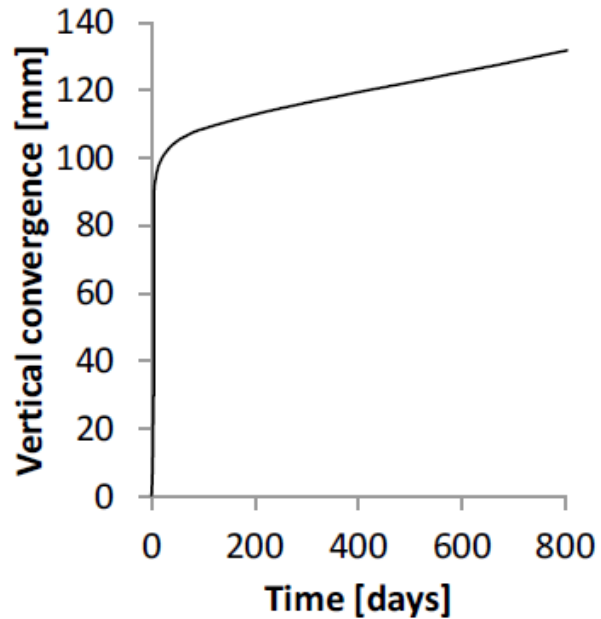
- Isotropic model :



4. Numerical modelling – Fractures modelling

4.2 Galery type 1 - Hydromechanical modelling :

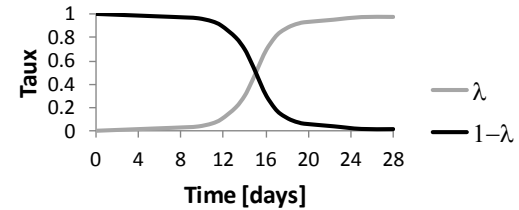
- Isotropic model :



4. Numerical modelling – Fractures modelling

4.2 Galery type 1 - Hydromechanical modelling :

- Anisotropic model :



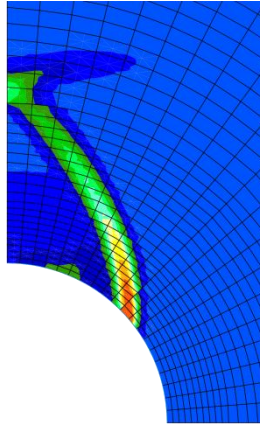
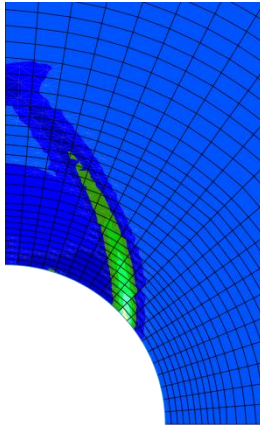
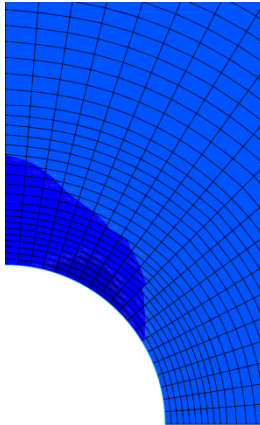
19.6 days

25 days

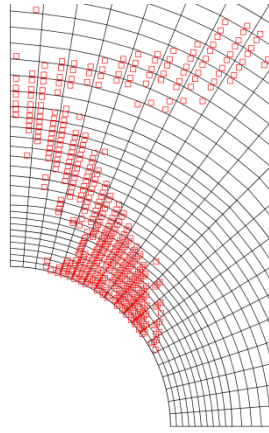
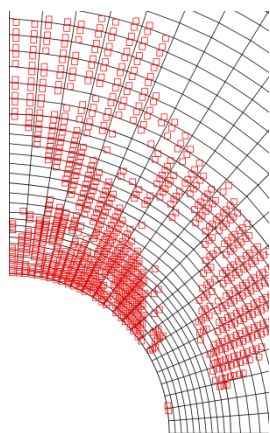
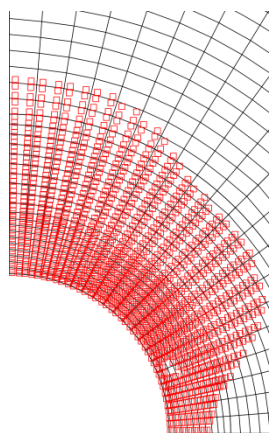
3 months

Total deviatoric strain

$$\varepsilon_{eq} = \sqrt{\frac{2}{3} \hat{\varepsilon}_{ij} \cdot \hat{\varepsilon}_{ij}}$$



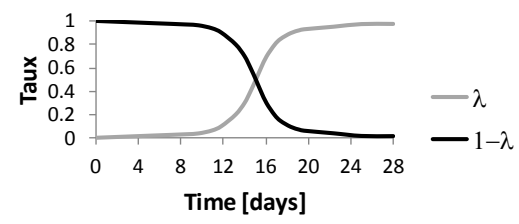
Plasticity



4. Numerical modelling – Fractures modelling

4.3 Galery type 2 - Hydromechanical modelling :

- Anisotropic model :

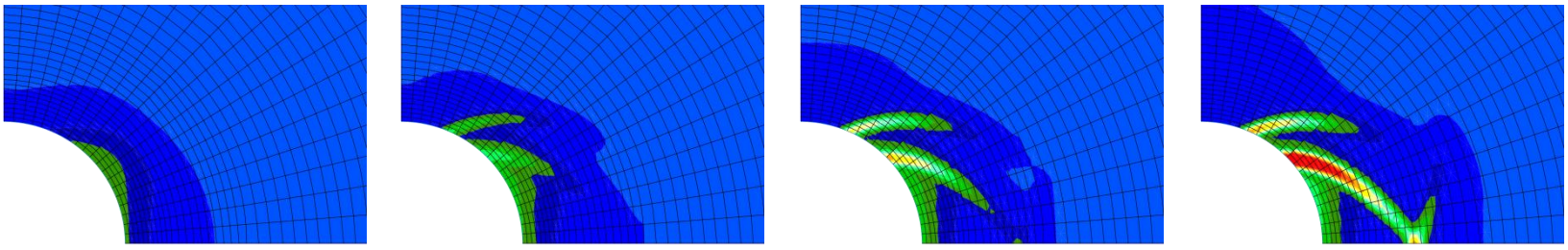


19.6 days 25 days 3 months 100 years

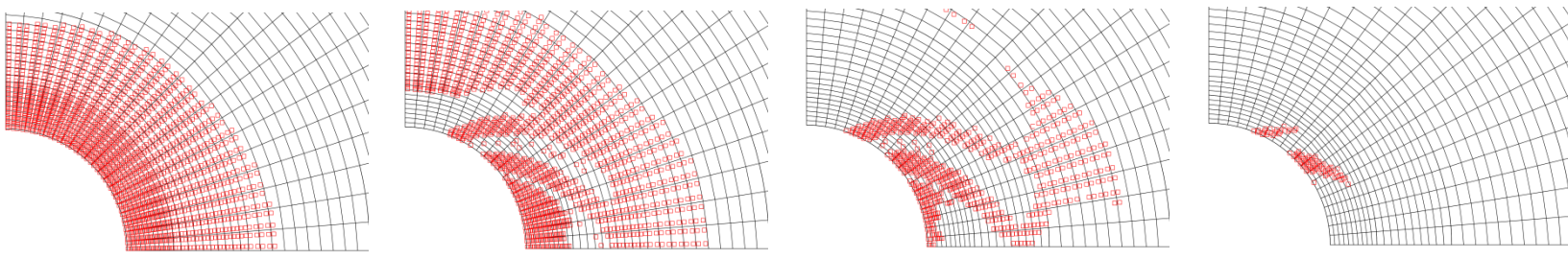
Total deviatoric strain

$$\varepsilon_{eq} = \sqrt{\frac{2}{3} \hat{\varepsilon}_{ij} \hat{\varepsilon}_{ij}}$$

0 0.030

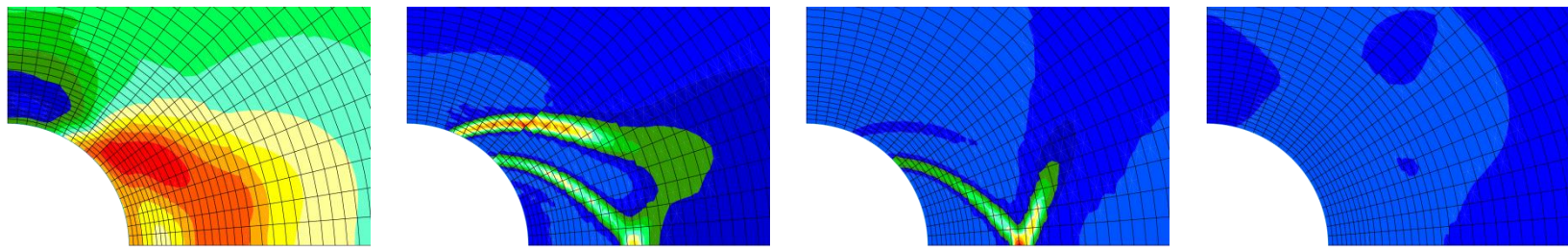


Plasticity

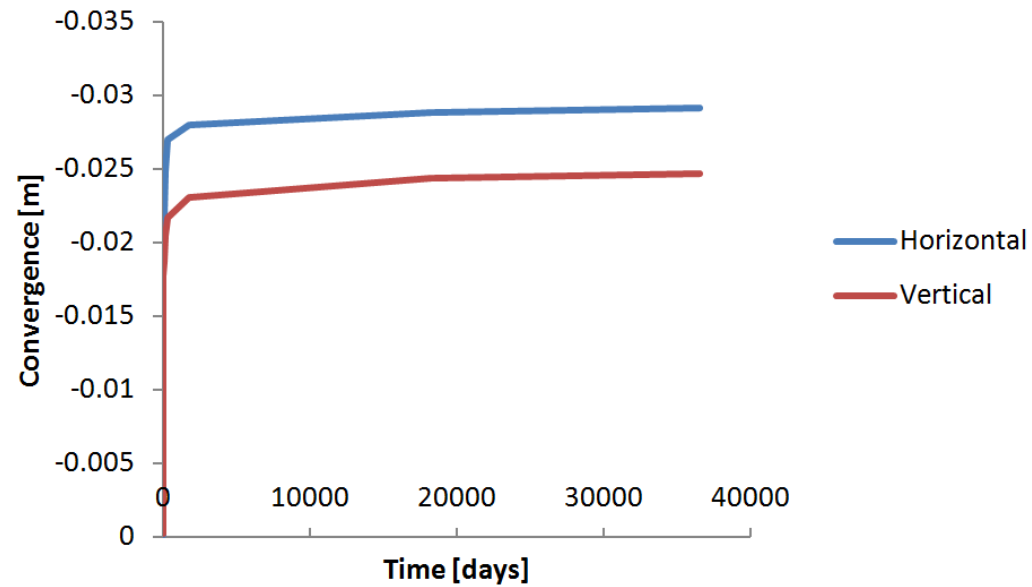


Deviatoric strain increment

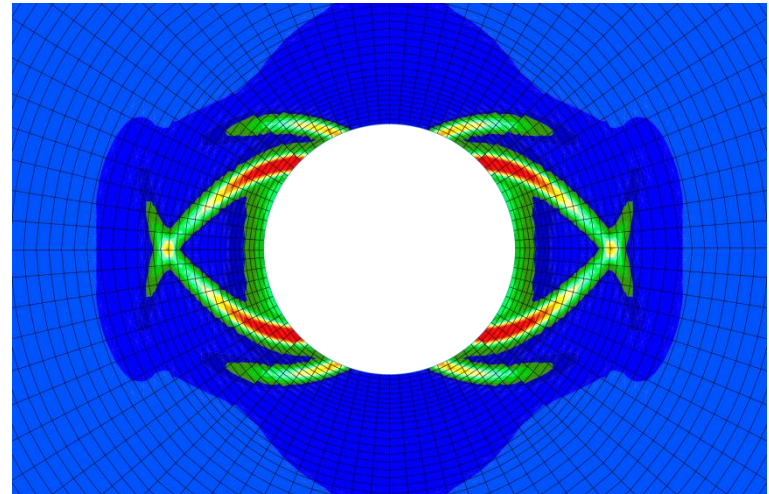
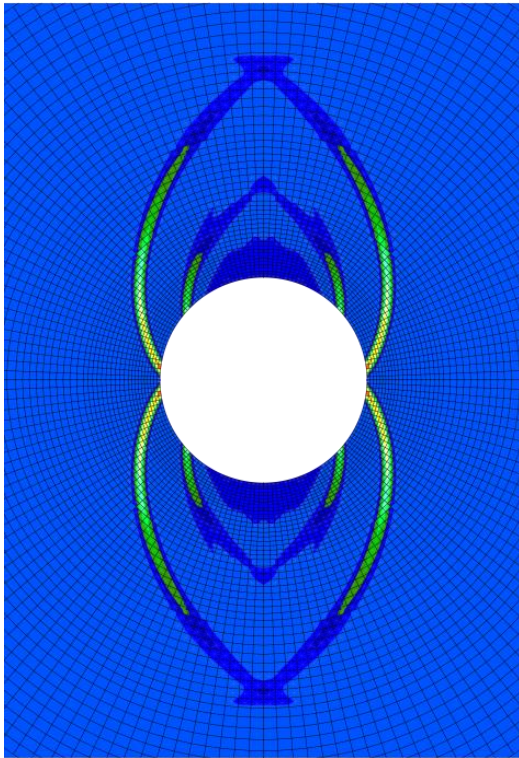
$$d\varepsilon_{eq}$$



4.3 Galery type 2 - Hydromechanical modelling :



4.3 Galery type 1 and 2 - Hydromechanical modelling :



1. CONSTITUTIVE MODELS
2. MODELS FITTING
3. NUMERICAL MODELLING – TYPE 1
4. NUMERICAL MODELLING – FRACTURES MODELLING – TYPE 1 AND 2
5. **CONCLUSIONS AND OUTLOOKS**

